

## Supplementary Information for

Translation-coupled RNA replication and parasitic replicators in  
membrane-free compartments

Ryo Mizuuchi\*, Norikazu Ichihashi

\*Email: mizuuchi@bio.c.u-tokyo.ac.jp

### **This PDF file includes:**

Supplementary Results  
Supplementary Discussion  
Materials and Methods  
Figs. S1 to S5  
Tables S1 to S3  
References

## Materials and Methods

**RNA preparation.** All the genomic RNAs (the round 128 clone,<sup>1</sup> R30,<sup>2</sup> and Host-99<sup>3</sup> clones) and the parasitic RNAs (Parasite- $\gamma$ 115<sup>3</sup> and S222<sup>4</sup>) were obtained as described previously. Briefly, R30 and Host-99 genomic RNAs are evolved variants of the round 128 clone. Parasite- $\gamma$ 115 is a parasitic RNA that appeared in our previous evolution experiment of the round 128 clone.<sup>3</sup> S222 was obtained as a *de novo* synthesized or contaminated RNA. The round 128 clone was used as the genomic RNA in all experiments except for two (Fig. 3E and Fig. 4, performed with R30 and Host-99, respectively). Parasite- $\gamma$ 115 was used as the parasitic RNA in all experiments except for one (Fig. S5C). All of the RNAs were prepared by *in vitro* transcription using T7 RNA polymerase (Takara, Japan) as described previously.<sup>5</sup> For fluorescent-labelled RNA synthesis, the transcription was conducted in the presence of Cyanine3 (Cy3)- or Cyanine5 (Cy5)-labeled UTP (PerkinElmer, USA).

**Preparation of aqueous two phase systems (ATPS) containing the translation-coupled RNA replication (TcRR) system.** Polyethylene glycol (PEG), dextran (DEX), and fluorescein isothiocyanate-dextran (FITC-DEX) were purchased from Sigma-Aldrich, USA. The average molecular weights of PEG, DEX, and FITC-DEX were 20 kDa, 9–11 kDa, and 10 kDa, respectively. The PEG and DEX were dissolved in water and stored as 40 wt% stock solutions. For some microscopic observation, the DEX stock solution contained 0.2 wt% FITC-DEX. The DEX was first mixed with a TcRR system, consisting of each RNA and the custom-made reconstituted translation system (Tables S1, S2), whose composition was slightly modified from the most recent TcRR system<sup>4</sup> (8 mM magnesium acetate (Mg(OAc)<sub>2</sub>) and 100 nM HrpA, instead of 16 mM and 63 nM, respectively). Then, PEG was added to the mixture of DEX and the TcRR system. The final compositions of the polymers were 15 wt% PEG and 1.5 wt% DEX. The sample was typically prepared as 15  $\mu$ l aliquots, and all procedures were conducted on ice. The DEX/PEG solutions were then vigorously mixed using a vortex mixer (Genie 2, Scientific Industries, USA) to obtain an ATPS, where DEX-rich phase droplets were dispersed in a continuous PEG phase.

**Microscopy.** Microscopic observations were performed with a TCS SP8 confocal laser scanning microscope (Leica, Wetzlar, Germany) and a 40 $\times$  oil immersion objective at 22 °C. FITC, Cy3, Cy5 were excited with 488 nm, 561 nm, and 633 nm lasers, respectively, and imaged at 490–540 nm, 570–630 nm, and 650–730 nm, respectively. Freshly prepared ATPS or ATPS incubated at 37 °C for the indicated time was immediately subjected to the microscopic observation. 26 nM Cy5-labeled genomic RNA and 260 nM Cy3-labeled parasitic RNA were used for microscopic observations. The obtained images of fluorescent DEX-rich phase droplets were analyzed using ImageJ (NIH); all signals with >10 pixel area and >0.8 circularity in each image were assumed as single droplets, and the size of each droplet was determined.

**Analysis of protein localization by SDS-polyacrylamide gel electrophoresis (SDS-PAGE).** A freshly prepared 30  $\mu$ l aliquot of the ATPS containing the TcRR system was centrifuged (2,000 g, 3 min) to obtain continuous DEX-rich and PEG-rich phases. 1  $\mu$ l of each phase was diluted with 9  $\mu$ l water, mixed with 40  $\mu$ l ice-cold acetone, and kept at –20 °C for 60 min. The mixtures were then centrifuged (15,000 g, 10 min) at 4 °C, followed by discarding of the supernatants to obtain precipitates. After evaporation of the

remaining acetone by air drying, the precipitates were solubilized in sodium dodecyl sulfate (SDS) sample buffer (50 mM Tris(hydroxymethyl)aminomethane Hydrochloride (Tris-HCl, pH 7.4), 2% SDS, 0.86 M 2-mercaptoethanol, and 10% glycerol) and subjected to SDS-PAGE using a 10–20% gradient gel (Funakoshi, Japan) followed by Coomassie Brilliant Blue staining.

**TcRR reaction.** The TcRR reaction was conducted in the absence or presence of ATPS, or in a continuous DEX 9–11 kDa or PEG 20 kDa phase, using different RNA concentrations as described in the main text. Some reactions were performed in 16 mM Mg(OAc)<sub>2</sub> instead of 8 mM Mg(OAc)<sub>2</sub> (Table S2) as described in the main text. After the incubation at 37 °C for the indicated times, each mixture was vigorously mixed using the vortex mixer, and an aliquot was subjected to quantitative PCR after reverse transcription (RT-PCR) to determine RNA concentrations, as described previously,<sup>1</sup> by using One Step TB Green<sup>®</sup> PrimeScript<sup>™</sup> PLUS RT-PCR Kit (Takara, Japan) except for Fig. 3E. Primers 1 and 2, primers 3 and 4, primers 5 and 6 (Table S3) were used as pairs in quantitative RT-PCR for the detection of the original genomic RNA (the round 128 clone), the parasitic RNA, and a genomic RNA variant (Host-99), respectively. In Fig. 3E, only the minus-strand of a genomic RNA variant (R30) was detected by using TB Green<sup>®</sup> Premix Ex Taq<sup>™</sup> II (Takara, Japan) with primer 7, and primers 8 and 9 for reverse transcription and following PCR, respectively. An aliquot of the TcRR reaction mixture was also subjected to 1% agarose gel electrophoresis followed by ethidium bromide staining.

**TcRR reaction in the presence of the known parasitic RNA.** ATPS, containing the genomic RNA, the parasitic RNA, both of the RNAs, or neither of the RNAs, were separately prepared. For each reaction, two of the ATPS (as shown in Fig. 3D) were gently mixed in a 19: 1 ratio so that the final concentration of the genomic and parasitic RNA was both 3 nM. The ATPS mixture was then incubated at 37 °C for the indicated times, and RNA concentrations were determined by quantitative RT-PCR as described above. Some reactions were performed without ATPS by simply incubating 3 nM of the genomic and parasitic RNAs in the TcRR system.

**RNA replication by purified Q $\beta$  replicase.** Q $\beta$  replicase was purified as described previously.<sup>7</sup> 300 nM Q $\beta$  replicase was mixed with the TcRR mixture (8 mM Mg(OAc)<sub>2</sub>, 0 mM amino acids to stop the translation of a genomic RNA) and incubated at 37 °C for 30 min in the presence or absence of ATPS, 10 nM of the genomic RNA, a varied concentration of a parasitic RNA (S222). Some reactions in ATPS were performed immediately after centrifuging the ATPS (15,000 g, 1 min). An aliquot of the reaction mixtures was subjected to 1% agarose gel electrophoresis followed by ethidium bromide staining. For some reactions, the concentrations of the genomic RNA were determined by quantitative RT-PCR as described above.

**TcRR reaction through the supplementation of CTP.** The TcRR reaction was performed in an ATPS as described above, using 10 nM of a genomic RNA variant (Host-99). The concentrations of all of the translation proteins (Table S1) were halved, and 62.5  $\mu$ M CTP was used instead of 1.25 mM CTP (Table S2). The ATPS mixture was then incubated at 37 °C for 5 h. At 2 h of the incubation, water or 625  $\mu$ M CTP (0.03 volume fraction of the

total mixture) was mixed with the ATPS. The RNA concentrations were measured by quantitative RT-PCR as described above.

## Supplementary Results

In Fig. 3D, we examined the replication of the genomic RNA in the presence of the parasitic RNA by manually separating the two RNAs into different ATPS compartments. However, as mentioned in the main text as well, in the evolution of a genetic RNA replicator, parasitic RNAs likely appear spontaneously through mutations in compartments where a genomic RNA already exists.<sup>3,8,9</sup> Here, we examined whether an ATPS can repress the replication of such a small amount of parasitic RNA without the manual segregation process. We first replicated the genomic RNA using purified Q $\beta$  replicase without the addition of known parasitic RNAs (Fig. S5A). The replication was performed in bulk (a), the ATPS (b), or the ATPS after centrifugation to induce droplet fusion (c). An agarose gel electrophoresis revealed that the appearance of parasitic RNA was prevented only in the ATPS without centrifugation (b). The extent of parasitic RNA replication was almost the same in bulk (a) and centrifuged ATPS (c). The same level of parasitic RNA was also observed in replication without adding the genomic RNA, meaning that the parasitic RNA could have been generated *de novo* (derived from existing RNAs such as tRNA and ribosomal RNA) or contaminated in the original reaction mixture, which cannot be distinguished. We also examined the replication of genomic RNA in conditions (a), (b), and (c) (Fig. S5B). We found that the genomic RNA replicated significantly better in condition (b) than condition (c), suggesting that the formation of droplets was critical to support RNA replication with purified replicase in the ATPS by preventing the amplification of the parasitic RNA.

A previous study characterized a dominant parasitic RNA that appears in the RNA replication with the purified replicase as a 222 nt short RNA, which was termed S222.<sup>4</sup> We therefore replicated varied concentrations of S222 using the purified replicase to estimate the maximum possible number of *de novo* synthesized or contaminated S222 in the ATPS (Fig. S5C). About 100 fM ( $6 \times 10^4$  molecules per 1  $\mu$ L) of S222 was required for its detection by agarose gel electrophoresis. Consistently, the droplet number in the ATPS was calculated to be roughly  $6 \times 10^4$ – $2 \times 10^5$  per 1  $\mu$ L by using mean diameters estimated in Fig. S3 and assuming that 10% volume of the ATPS is the DEX-rich phase. Thus, the prevention of parasitic RNA amplification in the ATPS could be explained by the effect of compartmentalization, such as resource limitation (e.g., replicase) in each compartment (Fig. S5D).

## Supplementary Discussion

As shown in Fig. 2A, B, and S1, changing the concentration of  $\text{Mg}(\text{OAc})_2$  from 16 mM to 8 mM was critical to stimulate the TcRR reaction in the ATPS. As the concentration of  $\text{Mg}(\text{OAc})_2$  slightly differed from its optimum inhibited protein synthesis by the PURE (protein synthesis using recombinant elements) system (the translation system in the TcRR system),<sup>10</sup> this improvement was perhaps because magnesium ions were concentrated in the DEX-rich phase droplets with the accumulation of RNA and proteins.

In the TcRR reaction performed with the pre-mixed genomic and parasitic RNAs (Fig. 3D, #1 and #4), the replication of the parasitic RNA relative to the genomic RNA was higher in the absence of the ATPS (#4) than in its presence (#1). One possibility to explain this result is efficient translation in the absence of the ATPS, considering the higher TcRR activity in bulk than in the ATPS (Fig. 2A, B). If a sufficient amount of  $\text{Q}\beta$  replicase was freely available, the difference in the replication of the genomic and parasitic RNA would increase exponentially until the RNAs sequester most of the replication enzymes.

As shown in Fig. 3B and C, we found that the inter-droplet diffusion of 510–2041 nt RNAs (and likely 222 nt RNA, as shown in Fig. S5) was prevented in the DEX-rich phase droplets of the ATPS. On the other hand, a previous study on a DEX/PEG ATPS showed the rapid exchange of short (15–50 nt) RNAs between DEX-rich phase droplets.<sup>11</sup> These differences may have resulted from the different lengths of investigated RNAs and the different compositions of DEX and PEG in ATPS. In fact, a previous study showed that an exponentially larger fraction of RNA localized in a DEX-rich phase of a DEX/PEG ATPS as the length of RNA increased.<sup>12</sup> On the other hand, the shortest length of a parasitic RNA that appeared and became dominant in our previous evolution experiment of the genomic RNA (the round 128 clone) was approximately 220 nt.<sup>3</sup> Our ATPS could therefore function as compartments for the sustainable replication and evolution of the genomic RNA, which should be examined in future studies.

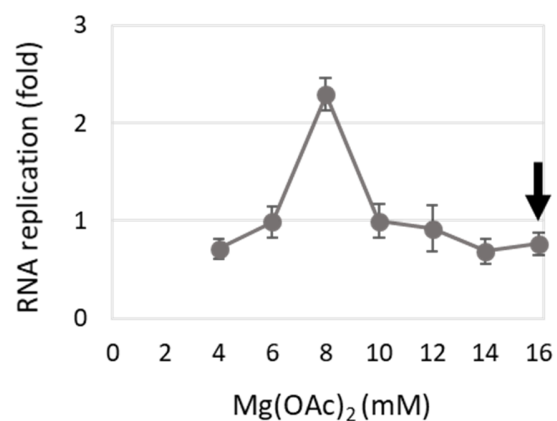


**Fig. S1.** Optimization of magnesium acetate concentration. The TcRR system with 3 nM genomic RNA in the ATPS was incubated in varied  $\text{Mg}(\text{OAc})_2$  concentrations at 37 °C for 2 h, and the RNA concentration was measured by quantitative RT-PCR. The error bars indicate standard errors ( $N = 4$ ). The arrow indicates the original  $\text{Mg}(\text{OAc})_2$  concentration (16 mM).

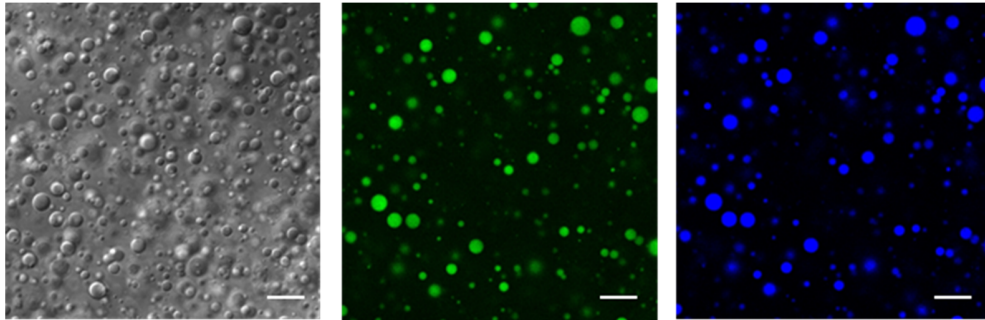


**Fig. S2.** Confocal microscope images of representative ATPS in 16 mM  $\text{Mg}(\text{OAc})_2$ . DEX 9–11 kDa and the genomic RNA were labeled with FITC and Cy5, respectively. Left panel: transmitted light. Middle panel: DEX fluorescence. Right panel: RNA fluorescence. Scale bar = 30  $\mu\text{m}$ .

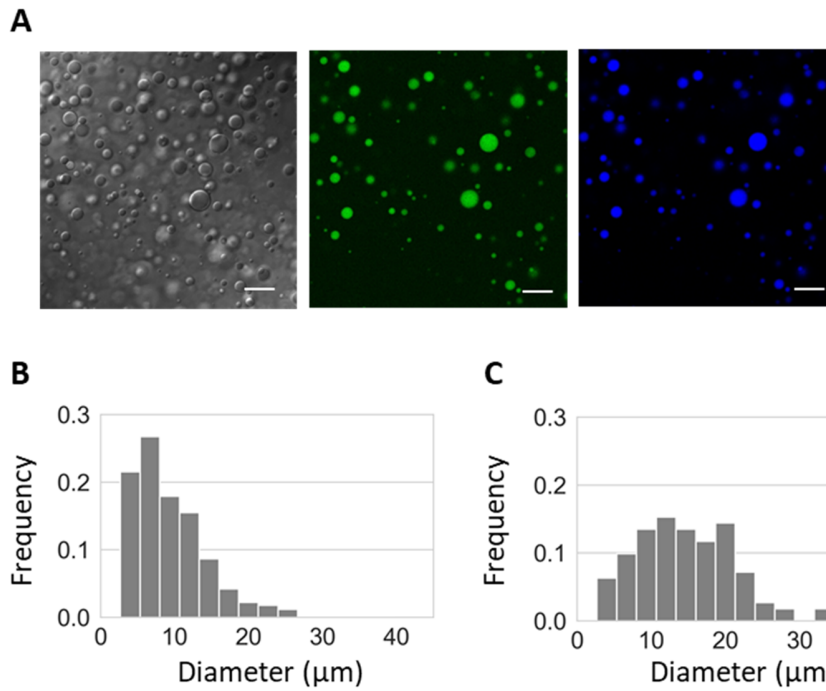


**Fig. S3.** Confocal microscope images of representative ATPS after 2 h incubation at 37 °C. DEX 10 kDa and the genomic RNA were labeled with fluorescein isothiocyanate (FITC) and Cy5, respectively. Left panel: transmitted light. Middle panel: DEX fluorescence. Right panel: RNA fluorescence. Scale bar = 30 μm. (B, C) The size distribution of DEX-rich phase droplets before (B) and after (C) incubation at 37 °C for 2 h, obtained from the image analysis. Droplets with FITC-labeled DEX were analyzed. The examples of analyzed images are shown in Fig. 1B (center) and Fig. S3A (center), respectively. The number of analyzed droplets was 497 and 111, respectively. The mean diameters were 9.5 and 15.1 μm, respectively.

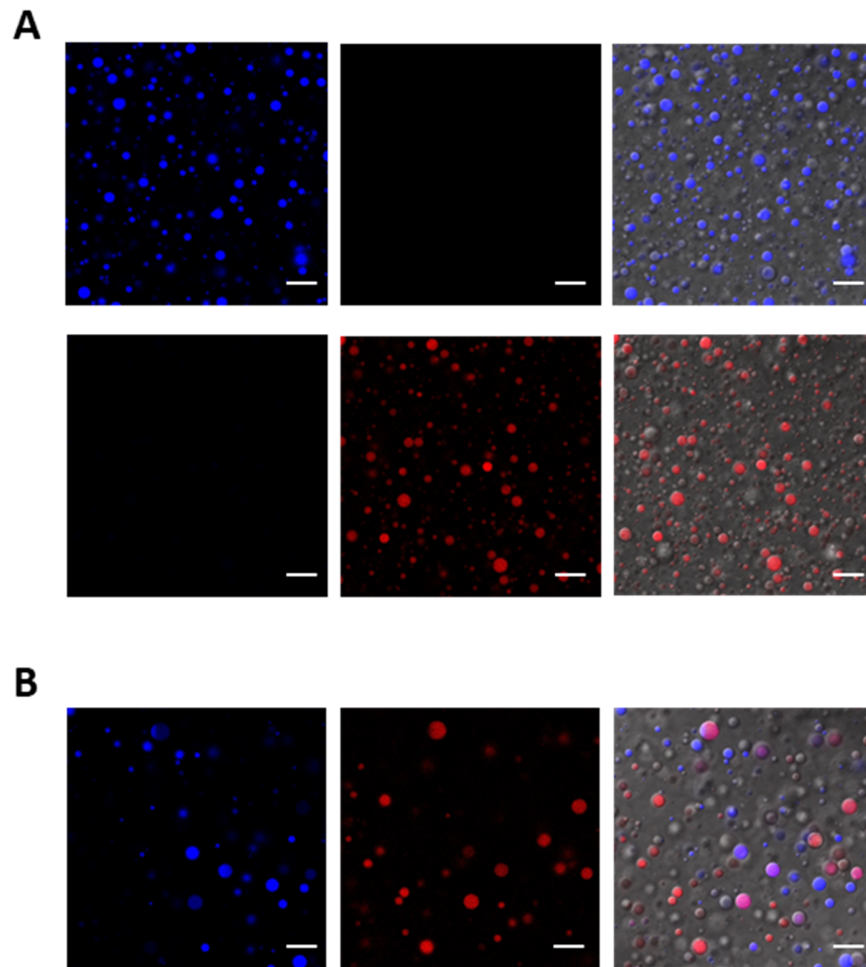


**Fig. S4.** (A) Confocal microscope images of representative ATPS, containing Cy5-genomic RNA (upper panels) or Cy3-parasitic RNA (lower panels). (B) Two separately prepared ATPS, one containing the Cy5-genomic RNA and one containing the Cy3-parasitic RNA, were mixed in a 1:1 ratio and imaged after the incubation at 37 °C for 2 h. For all rows, left panel: Cy5 fluorescence. Middle panel: Cy3 fluorescence. Right panel: both fluorescence images merged with the transmitted light image. All scale bars = 30  $\mu$ m.

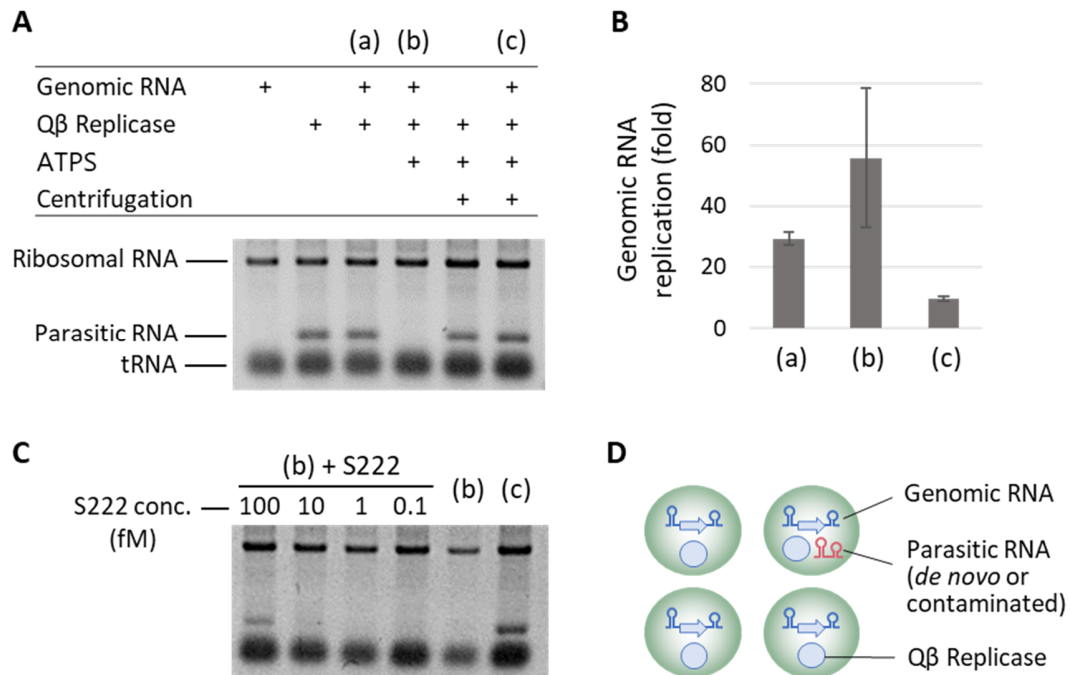


**Fig. S5.** RNA replication using purified Q $\beta$  replicase. (A) Various reaction mixtures as shown on the top were incubated at 37 °C for 30 min and were subjected to 1% agarose gel electrophoresis. The concentrations of the genomic RNA and the purified replicase were 3 nM and 300 nM, respectively. Conditions (a), (b), and (c) were further analyzed. (B) The replication of the genomic RNA, determined by quantitative RT-PCR. The error bars indicate standard errors (N = 3). (C) RNA replication with varied concentrations of additional S222 parasitic RNA in condition (b). 1% agarose gel electrophoresis was performed after RNA replication at 37 °C for 30 min. (D) Illustration of how the ATPS could have prevented the replication of the parasitic RNA.

**Table S1.** Protein components of the reconstituted translation system

Name	Molecular weight (kDa)	Concentration (nM)	Names	Molecular weight (kDa)	Concentration (nM)
Initiation factor 1	8.1	25000	Isoleucyl-tRNA synthetase	104	370
Initiation factor 2	97.3	1000	Leucyl-tRNA synthetase	97.2	41
Initiation factor 3	20.6	4900	Lysyl-tRNA synthetase	57.4	120
Elongation factor G	77.5	1100	Methionyl-tRNA synthetase	76.1	110
Elongation factor Tu	43.2	80000	Phenylalanyl-tRNA synthetase*	36.8, 87.4	130
Elongation factor Ts	30.3	3300	Prolyl-tRNA synthetase	63.7	170
Release factor 1	40.5	49	Seryl-tRNA synthetase	48.4	78
Release factor 2	41.3	48	Threonyl-tRNA synthetase	74	84
Release factor 3	59.4	170	Tryptophanyl-tRNA synthetase	37.4	28
Ribosome recycling factor	20.6	3900	Tyrosyl-tRNA synthetase	47.4	150
Alanyl-tRNA synthetase	96	730	Valyl-tRNA synthetase	108.2	17
Arginyl-tRNA synthetase	64.6	31	Methionyl-tRNA formyltransferase	34	590
Asparaginyl-tRNA synthetase	52.4	420	Myokinase	21.6	1400
Asparagyl-tRNA synthetase	65.9	120	Creatine kinase	43	250
Cysteinyl-tRNA synthetase	52.2	24	Nucleoside diphosphate kinase	15.3	16
Glutaminyl-tRNA synthetase	63.3	60	Pyrophosphatase	32.2	41
Glutamyl-tRNA synthetase	53.8	230	Trigger factor	48.2	1000
Glycyl-tRNA synthetase*	34.8, 76.8	86	ATP-dependent RNA helicase HrpA	145.8	100
Histidyl-tRNA synthetase	46.9	85	Ribosome*	4.4–61	1000

\*Glycyl-tRNA synthetase, phenylalanyl-tRNA synthetase, and ribosome consist of multiple subunits.

**Table S2.** Composition of non-protein components of the reconstituted translation system

Name	Concentration
Tyrosine	0.3 mM
Cysteine	0.3 mM
18 other amino acids	0.36 mM each
tRNA mix (Roche)	1.56 µg/µL
ATP	3.75 mM
GTP	2.5 mM
CTP	1.25 mM
UTP	1.25 mM
N-2-Hydroxyethylpiperazine-N <sup>1</sup> -2-ethanesulfonic acid (pH 7.6)	100 mM
Glutamic acid potassium salt	70 mM
Spermidine	0.375 mM
Magnesium acetate	8 mM*
Creatine phosphate	25 mM
Dithiothreitol	6 mM
10-Formyl-5,6,7,8-tetrahydrofolic acid	10 ng/µl

\*Optimized for the TcRR reaction in the ATPS. The original concentration was 16 mM.

**Table S3.** List of primers (from 5' end to 3' end)

---

Primer 1	ATACACATGGCTCGTAGAAAA
Primer 2	GGCGTACACGCTTGCGGAAGT
Primer 3	TAAGAAGGAGATATGCTTTAACGAA
Primer 4	TAGATCTCTCGAGTCTTGAAGGAC
Primer 5	GCTGCCTAACAGCTGCGAC
Primer 6	CGCTCTGGTCCCTTGTATG
Primer 7	TAAGCGAATGTTGCGAGCACGGCCCATTCTG TGACCTCAAG
Primer 8	GATCCACCCGCGGTTTTTC
Primer 9	TAAGCGAATGTTGCGAGCAC

---

## References

- 1 N. Ichihashi, K. Usui, Y. Kazuta, T. Sunami, T. Matsuura and T. Yomo, *Nat. Commun.*, 2013, **4**, 2494.
- 2 R. Mizuuchi, N. Ichihashi, K. Usui, Y. Kazuta and T. Yomo, *ACS Synth. Biol.*, 2015, **4**, 292–298.
- 3 T. Furubayashi, K. Ueda, Y. Bansho, M. Daisuke, N. Shota, R. Mizuuchi and N. Ichihashi, *Elife*, 2020, **9**, e56038.
- 4 K. Hosoda, T. Matsuura, H. Kita, N. Ichihashi, K. Tsukada and T. Yomo, *J. Biol. Chem.*, 2007, **282**, 15516–15527.
- 5 M. Yumura, N. Yamamoto, K. Yokoyama, H. Mori, T. Yomo and N. Ichihashi, *PLoS One*, 2017, **12**, 1–14.
- 6 R. Mizuuchi, N. Ichihashi and T. Yomo, *ChemBioChem*, 2016, **17**, 1229–1232.
- 7 H. Kita, J. Cho, T. Matsuura, T. Nakaishi, I. Taniguchi, T. Ichikawa, Y. Shima, I. Urabe and T. Yomo, *J. Biosci. Bioeng.*, 2006, **101**, 421–426.
- 8 S. Matsumura, Á. Kun, M. Ryckelynck, F. Coldren, A. Szilágyi, F. Jossinet, C. Rick, P. Nghe, E. Szathmáry and A. D. Griffiths, *Science*, 2016, **354**, 1293–1296.
- 9 R. Mizuuchi and N. Ichihashi, *Nat. Ecol. Evol.*, 2018, **2**, 1654–1660.
- 10 T. Matsuura, Y. Kazuta, T. Aita, J. Adachi and T. Yomo, *Mol. Syst. Biol.*, 2009, **5**, 1–10.
- 11 T. Z. Jia, C. Hentrich and J. W. Szostak, *Orig. Life Evol. Biosph.*, 2014, **44**, 1–12.
- 12 C. A. Strulson, R. C. Molden, C. D. Keating and P. C. Bevilacqua, *Nat. Chem.*, 2012, **4**, 941–946.
- 13 Y. Bansho, T. Furubayashi, N. Ichihashi and T. Yomo, *Proc. Natl. Acad. Sci. U. S. A.*, 2016, **113**, 4045–4050.